© 2016. Published by The Company of Biologists Ltd | Development (2016) 143, 950-961 doi:10.1242/dev.131573

The transcription factor SOX6 contributes to the developmental origins of obesity by promoting adipogenesis

Shi Chi Leow[1], Jeremie Poschmann[2], Peh Gek Too[1], Juan Yin[3], Roy Joseph[1], Craig McFarlane[1], Shaillay Dogra[1], Asim Shabbir[4], Philip W. Ingham[3,5], Shyam Prabhakar[2], Melvin K. S. Leow[1,6], Yung Seng Lee[1,7], Kai Lyn Ng[8], Yap Seng Chong[1,8], Peter D. Gluckman[1,9] and Walter Stünkel[1,*]

ABSTRACT

An association between impaired fetal growth and the postnatal development of obesity has been established. Here, by comparing adipocytes differentiated from mesenchymal stem cells (MSCs) taken from the umbilical cord and derived from normal and growth-restricted neonates, we identified the transcription factor SOX6 as highly expressed only in growth-restricted individuals. We found that SOX6 regulates adipogenesis in vertebrate species by activating adipogenic regulators including PPARγ, C/EBPα and MEST. We further show that SOX6 interacts with β-catenin in adipocytes, suggesting an inhibition of WNT/β-catenin signaling, thereby promoting adipogenesis. The upstream regulatory region of the *MEST* gene in MSCs from growth-restricted subjects harbors hypomethylated CpGs next to SOX6 binding motifs, and we found that SOX6 binding is impaired by adjacent CpG methylation. In summary, we report that SOX6 is a novel regulator of adipogenesis synergizing with epigenetic mechanisms.

KEY WORDS: Developmental origins, Epigenetics, Fetal growth restriction, Mesenchymal stem cells, Obesity, Transcription factor, Human, Mouse, Zebrafish

INTRODUCTION

Obesity is becoming increasingly prevalent and contributes to morbidity and mortality worldwide (Ng et al., 2014; Bhurosy and Jeewon, 2014). Although there is little doubt that it can result from adult lifestyle factors, there is increasing evidence for developmental factors playing an important role and these appear to operate through epigenetic pathways (van Dijk et al., 2015). Indeed, there is compelling evidence to support the concept that the origins of obesity often begin *in utero* (Desai et al., 2005; de Rooij et al., 2007) and impaired fetal growth has been linked to the development of obesity and metabolic diseases in adult life (Godfrey and Barker, 2001; Kensara et al., 2006). The role of low birth weight in the development of human adult non-communicable diseases has been described (Lackland et al., 2000; Tian et al., 2006). In particular, infants with low birth weight and fetal growth restriction combined with accelerated catch-up in the first few years of life are at higher risk of developing obesity (Khandelwal et al., 2014; Varvarigou, 2010).

The mechanistic pathway by which impaired intrauterine conditions induce later sensitivity to an obesogenic environment has been extensively reviewed (Hanson and Gluckman, 2014) and there is clinical evidence suggesting that epigenetic mechanisms are involved (Godfrey et al., 2011). To explore molecular mechanisms that might be important in this relationship, we previously reported the use of multipotent mesenchymal stem cells (MSCs) from the Wharton's jelly of umbilical cord (UC) tissue to generate primary UC-MSC isolates from small for gestational age (SGA) and normal neonates (Sukarieh et al., 2014). Chromatin immunoprecipitation-sequencing (ChIP-seq) studies from adipocytes differentiated from MSCs revealed candidate genes that were found to be associated with histone hyperacetylation and increased gene expression in the SGA group (Joseph et al., 2015). One gene of uncertain functional importance found in that study is *SOX6* [SRY (sex determining region Y)-box 6]. Here, we describe the effects of SOX6 on adipogenesis and demonstrate putative molecular mechanisms by showing that SOX6 regulates the expression of key adipogenic regulators and synergizes with epigenetic pathways involving MEST (mesoderm specific transcript), which is known to be associated with adipocyte size (Takahashi et al., 2005) and adipose tissue expansion but with as yet unknown biochemical functions (Voigt et al., 2015). Epigenetic changes within the *MEST* promoter have previously been associated with maternal stress leading to adverse birth outcomes (Vidal et al., 2014). Our results show that epigenetic properties of the *MEST* gene upstream regulatory region synergize with SOX6 function in positively regulating adipogenesis in MSCs isolated from SGA individuals.

RESULTS

SOX6 is highly expressed in MSC-derived adipocytes from SGA neonates

In our previous study, histone ChIP-seq using preadipocytes (cycle 0), intermediate adipocytes (cycle 3) and mature differentiated adipocytes (cycle 6) from two representative cell lines of SGA (MSC-01) and control group (MSC-44) of human neonates revealed notably different enrichment of H3K27 acetylation sites in adipocytes derived from the SGA background (Joseph et al., 2015). *SOX6* was among the most significant genes with promoter-associated H3K27 acetylation along with lower levels of H3K27 trimethylation in adipocytes derived from the MSC-01 SGA compared with the MSC-44 control isolate (Fig. 1A).

We evaluated the expression pattern of *SOX6* in adipocytes derived from both MSC-01 and MSC-44 (Fig. 1B), as well as adipocytes derived from an extended larger group of primary SGA

[1]Singapore Institute for Clinical Sciences (SICS), Agency for Science Technology and Research (A*STAR), 30 Medical Drive, Singapore, Singapore 117609. [2]Genome Institute of Singapore, Agency for Science Technology and Research (A*STAR), Singapore, Singapore 138672. [3]Lee Kong Chian School of Medicine, Nanyang Technological University, Singapore, Singapore 636921. [4]Department of Surgery, National University Hospital, National University of Singapore, Singapore 119074. [5]Developmental and Biomedical Genetics Laboratory, Institute of Molecular and Cell Biology, Agency for Science Technology and Research (A*STAR), Singapore, Singapore 138673. [6]Department of Endocrinology, Tan Tock Seng Hospital, Singapore, Singapore 308433. [7]Department of Paediatrics, Yong Loo Lin School of Medicine, National University of Singapore, Singapore 119228. [8]Department of Obstetrics and Gynaecology, Yong Loo Lin School of Medicine, National University of Singapore, Singapore 119228. [9]Liggins Institute, University of Auckland, Auckland 1142, New Zealand.

*Author for correspondence (walter_stunkel@sics.a-star.edu.sg)

Received 6 October 2015; Accepted 5 February 2016

Development (2016) 143, 950-961 doi:10.1242/dev.131573

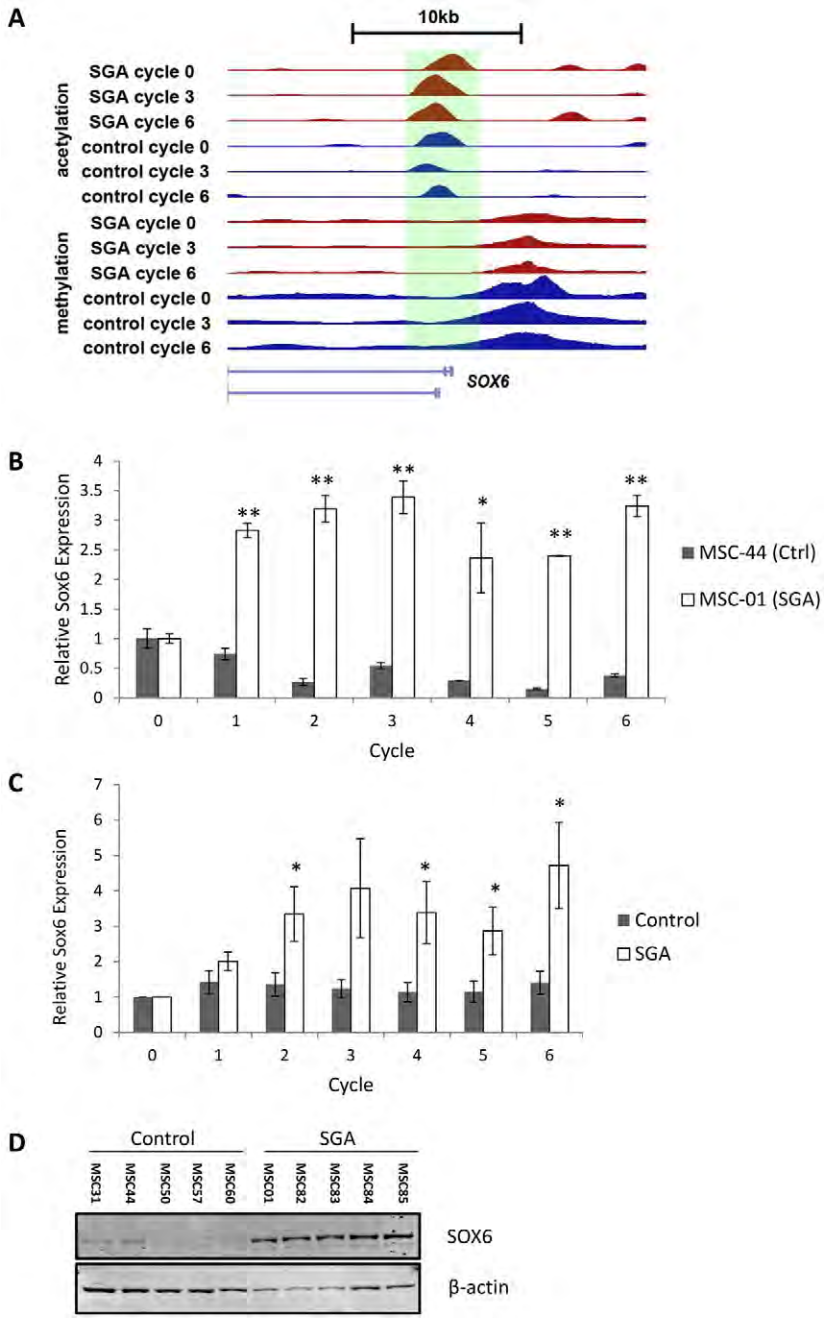

Fig. 1. Higher expression of SOX6 in mature adipocytes derived from SGA MSCs. (A) UCSC genome browser view of SGA (MSC-01, red) and control (MSC-44, blue) H3K27 acetylation and trimethylation ChIP-seq signals around the human *SOX6* gene locus. Shown are wiggle tracks of normalized read counts. The two blue arrows indicate the gene starts of SOX6 and a SOX6 isoform, as well as length and direction. The green shaded area depicts the promoter peak. (B) mRNA expression levels of *SOX6* in adipocytes from SGA compared with control as determined by qRT-PCR. Results are representative of three independent experiments. Data are shown as mean fold change±s.e.m. for *SOX6* expression relative to that of the MSC-44 cycle 0 sample. A two-way ANOVA analysis was performed to show a significant difference in the effect of differentiation cycles (P<0.0001) and MSC lines (P<0.0001) for gene expression between biological repeats followed by Student's *t*-test (*P<0.05, **P<0.01). (C) *SOX6* mRNA expression in an extended group of SGA (n=8) and control (n=5) MSC lines. Data are shown as mean fold change±s.e.m. for *SOX6* expression relative to control lines at cycle 0. A two-way ANOVA analysis was performed to show a significant difference in the effect of differentiation cycles (P=0.0493) and sample groups (P<0.0001) for gene expression between MSC lines followed by a Student's *t*-test (*P<0.05). (D) SOX6 protein expression is significantly higher in mature adipocytes from SGA-derived MSCs.

and control MSC isolates (Fig. 1C, Table S2). *SOX6* gene expression levels were significantly higher in adipocytes from the SGA background. Similar observations were made for known adipogenic genes, such as those encoding PPARγ, C/EBPα, FABP4 and FASN (Fig. S1C), in line with our published observations of a higher adipogenic potential for differentiated MSCs derived from the SGA group (Joseph et al., 2015). Western blots showing the protein levels of SOX6 in the adipocytes (Fig. 1D) confirmed our qRT-PCR findings and correlated well with the transcriptional state predicted by the ChIP-seq data set.

Modulation of SOX6 expression regulates adipocyte differentiation and triglyceride levels

A function for SOX6 in human adipocyte differentiation had not been reported previously and, in order to test the hypothesis that SOX6 exerts an effect on adipocyte differentiation, we performed siRNA-mediated SOX6 knockdown experiments with several differentiated primary human Wharton's jelly-derived MSC lines as well as adipose stromal cell (ASC) lines. Silencing SOX6 expression reduced the formation of lipid droplets in both human cell lines (MSC-01 and APOD-01, Fig. 2A,B). These results were concordant with triglyceride levels measured in the same samples (Fig. 2C,D). Similar results were obtained in mouse 3T3L1 adipocytes (Fig. S1A), as well as in additional human ASC and MSC lines (Fig. S1B, Fig. S2A, Table S2). We also applied the reverse approach by transfecting a SOX6 expression vector into 3T3L1 preadipocytes and observed a significant increase in cellular triglyceride levels compared with the GFP control vector at day 4 of adipogenesis (Fig. S1D).

To confirm that the inhibition of adipogenesis was specifically due to SOX6 inhibition, we measured the mRNA expression of

Development (2016) 143, 950-961 doi:10.1242/dev.131573

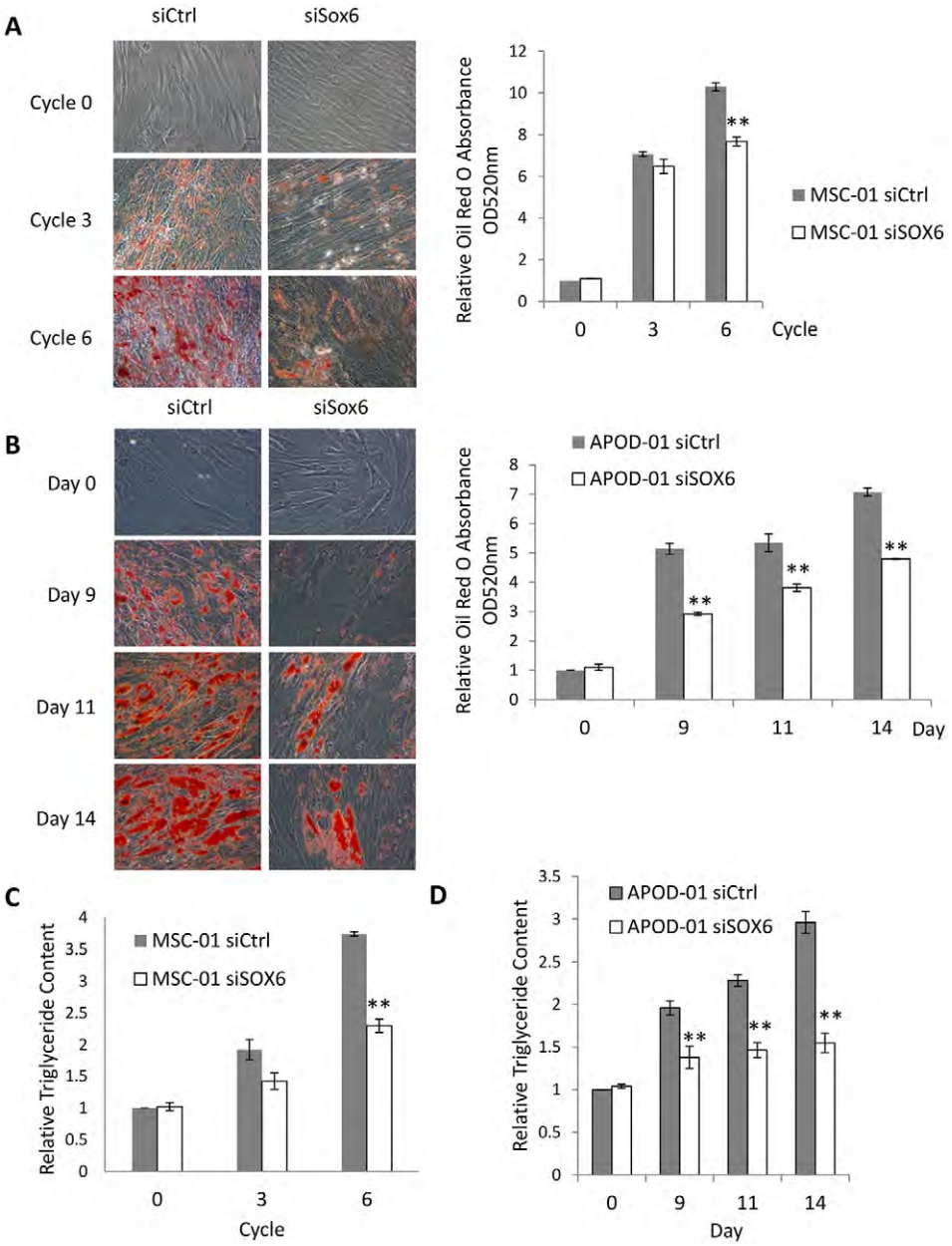

Fig. 2. SOX6 downregulation impairs adipogenesis. (A,B) Human MSC-01 and APOD-01 cells at different stages of differentiation. Images are representatives of three independent experiments. Quantification of Oil Red O absorption by spectrophotometry is shown to the right. Data represent the mean relative absorbance±s.e.m. compared with siCtrl cycle/day 0 (n=3, $^{**}P$<0.01). (C,D) The amount of total triglycerides in siCtrl-treated or siSOX6-treated MSC-01 and APOD-01 cells were measured in triplicate and normalized to their total protein content in three separate experiments. Data are shown as mean±s.e.m. relative to siCtrl cycle/day 0. A two-way ANOVA was performed to show a significant difference between time points (P<0.0001) and between siRNA treatment (P<0.0001 for MSC-01 and APOD-01) over triglyceride content followed by a Student's t-test ($^{**}P$<0.01).

other SOX family members, such as *SOX5*, *SOX9* and *SOX13*, following the siRNA-mediated SOX6 depletion. As shown in Fig. S2B,C, inhibition of SOX6 did not lead to significant changes in the expression of other members of the SOX family.

SOX6 enhances adipogenesis by directly regulating the expression of adipogenic genes

In order to gain mechanistic insights into the effects of SOX6 on adipogenesis, we examined the expression patterns of key adipocyte markers in fully differentiated adipocytes. Knockdown of SOX6 led to a reduction in the expression of genes encoding MEST, FABP4, FASN, GLUT4 (SLC2A4), PPARγ and C/EBPα in MSC-01 cells (Fig. 3A-C), in all ASC-derived adipocytes (Fig. S3A,B) and in mouse 3T3L1 cells (Fig. S4A,B). The transcription factors PPARγ and C/EBPα are crucial for adipogenesis (Rosen et al., 2002) and their expression is dependent on that of adipogenic initiation factors including C/EBPβ and C/EBPδ. Quantitative PCR analyses showed that the gene encoding C/EBPβ was downregulated by SOX6 depletion in MSC-01 at cycle 0 (Fig. 3B), in ASC lines (Fig. S3A,B, right panels) and in 3T3L1 preadipocytes (Fig. S4A, right panel). C/EBPδ expression was not affected in MSC-01 and 3T3L1 cells, but significantly downregulated in the adult human ASC lines (Fig. S3A,B, right panels). These findings indicate that SOX6 mediates adipocyte differentiation and lipogenesis by upregulating the adipogenic signaling cascade, specifically increasing adipocyte expression of PPARγ, C/EBPα, FABP4 and MEST.

In light of our earlier findings, we further examined whether SOX6 can directly regulate the expression of MEST and PPARγ by performing ChIP using preadipocytes (cycle 0/day 0), intermediate adipocytes (cycle 3/day 4) and mature differentiated adipocytes (cycle 6/day 8) derived from MSC-01 and 3T3L1 cells. Allowing one base deviation from the consensus SOX6 binding motif (WWCAAWG), we identified 17 potential SOX6 binding sites 1 kb upstream of the *MEST* gene and designed three sets of primers to test selected sites (Fig. 3D) in MSC-01 cells. We confirmed that, under differentiating conditions, SOX6 is enriched at the *MEST* promoter

Development (2016) 143, 950-961 doi:10.1242/dev.131573

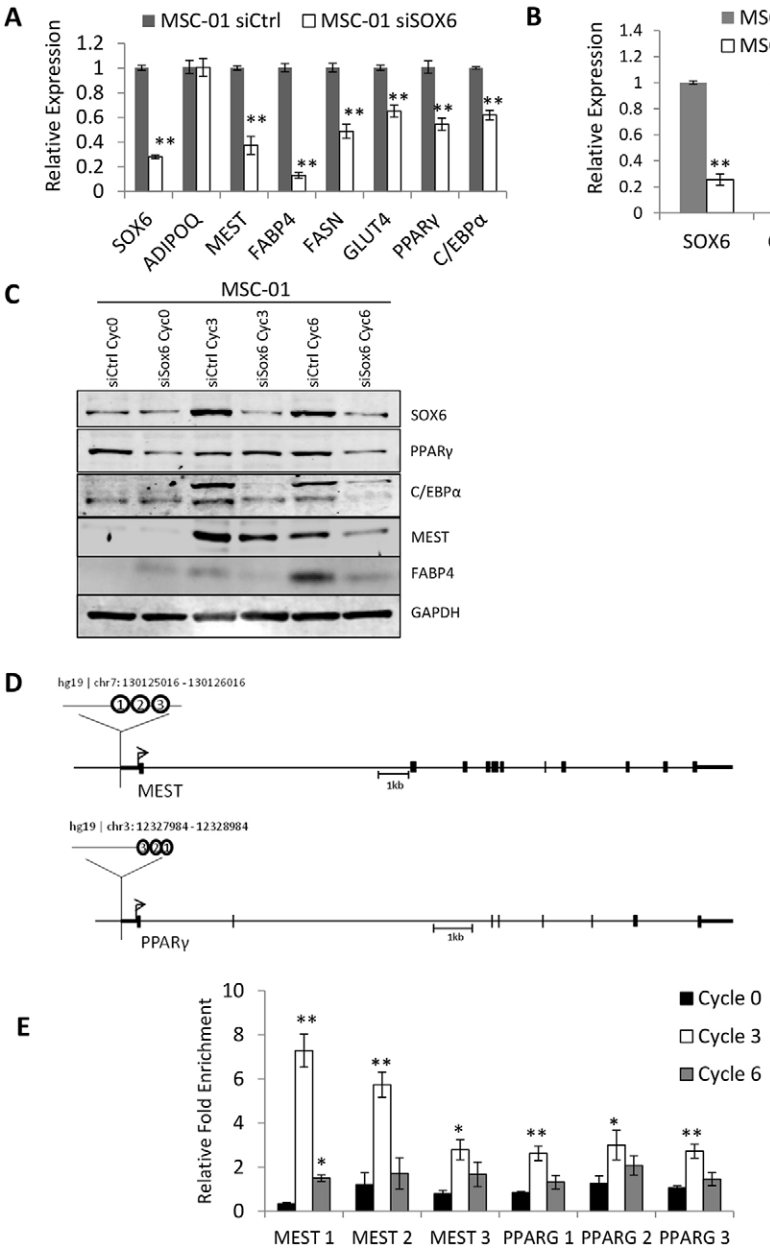

Fig. 3. SOX6 regulates the expression of key adipogenic genes. (A,B) mRNA expression levels of genes encoding the adipocyte markers ADIPOQ, MEST, FABP4, FASN, GLUT4 and the adipogenic regulators PPARγ, C/EBPα, C/EBPβ and C/EBPδ were determined by qRT-PCR in siSOX6-treated MSC-01 cells in comparison with the control group (siCtrl) at cycle 6 of adipocyte differentiation. Data are shown as mean± s.e.m. of three independent experiments. $^{**}P<0.01$, Student's *t*-test. (C) Protein expression of SOX6 and adipogenic markers in siCtrl-treated and siSOX6-treated MSC-01 cells. (D,E) SOX6 enrichment at the *MEST* and *PPARG* promoters was measured by ChIP-qPCR at cycles 0, 3 and 6 of adipocyte differentiation in MSC-01 cells. Data are shown as mean fold enrichment±s.e.m. of three independent experiments and were normalized against IgG enrichment and against a negative control site (SOX4). $^{*}P<0.05$, $^{**}P<0.01$, Student's *t*-test.

region (Fig. 3E). Similarly, we observed stronger enrichment of SOX6 at the *Mest* promoter region in differentiating 3T3L1 cells as compared with fully differentiated cells at day 8 (Fig. S4C). Our ChIP analysis also demonstrated that endogenous SOX6 binds to the *PPARG* promoter region (Fig. 3E, Fig. S4C), indicating that this gene is also a direct downstream target of SOX6. In order to further support the hypothesis that SOX6 directly regulates expression of the genes encoding MEST and PPARγ by direct promoter binding, we conducted gene-specific luciferase reporter assays during the differentiation of 3T3L1 cells. siRNA-mediated SOX6 knockdown reduced both *Mest* and *Pparg* reporter gene activity (Fig. S4D,E).

CpGs within the *MEST* promoter are hypomethylated in differentiated adipocytes from SGA neonates and facilitate the binding of SOX6

Having established a role of SOX6 as an activator of adipogenesis, we aimed to gain insight into the mechanisms of SOX6 action in the context of the developmental induction of a propensity to obesity. We specifically addressed the question of whether potential synergisms between SOX6 overexpression and other molecular pathways can be found in Wharton's jelly-derived MSCs.

There are numerous examples demonstrating an impairment of transcription factor binding by site-specific CpG methylation (Cho et al., 2013). In order to investigate whether similar mechanisms exist for some of the downstream targets of SOX6, we assessed the methylation status of CpG dinucleotides adjacent to putative SOX6 binding sites within the *MEST* upstream regulatory region. As depicted in Fig. 4A, we selected six candidate sites (CpGs A-F) near the *MEST* transcriptional start site surrounding three putative SOX6 binding sites and determined their methylation status by pyrosequencing. We compared five adipocyte cell lines differentiated from Wharton's jelly MSCs taken from the control group and seven corresponding lines from the SGA group. All CpG sites showed a significant decrease in methylation levels in the SGA group compared with the controls (Fig. 4B). Hypomethylation

Development (2016) 143, 950-961 doi:10.1242/dev.131573

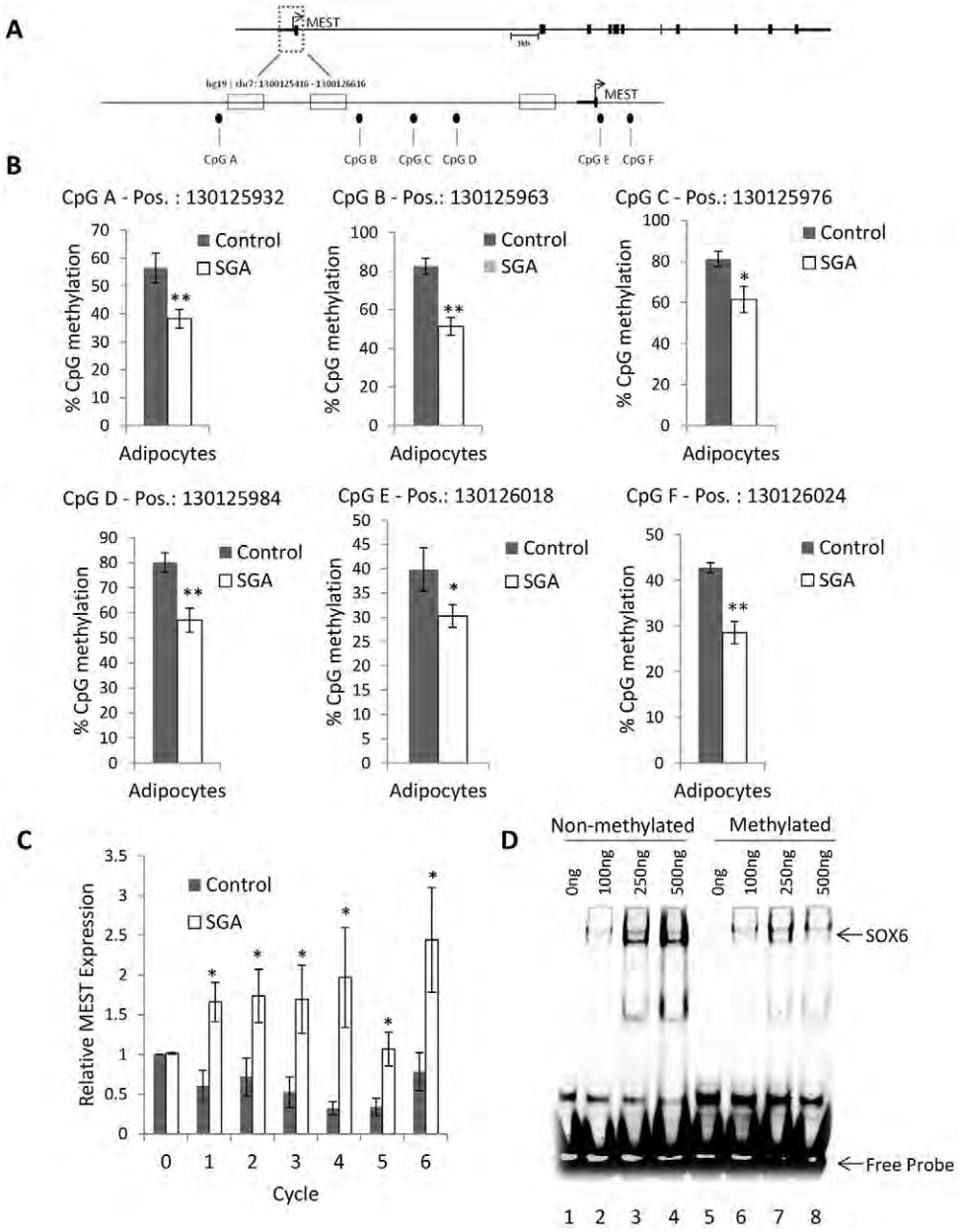

Fig. 4. CpGs next to SOX6 binding sites within the *MEST* upstream regulatory region are hypomethylated in SGA-derived differentiated adipocytes and CpG methylation interferes with SOX6 binding. (A) Map of the human *MEST* region next to the transcriptional start site covering three SOX6 binding sites (open boxes) surrounded by six CpGs (filled circles), which were selected for pyrosequencing. (B) Percentage of CpG methylation for each of the six individual CpGs described in A. Genomic locations of CpGs A-F are given above each bar chart. A group of control adipocyte lines (n=5) were compared with those from a group of SGA lines (n=7). Data are presented as mean±s.e.m. $^{**}P<0.01$, $^{*}P<0.05$, Student's t-test. (C) *MEST* mRNA expression in the group of SGA (n=7) and control (n=5) MSC lines as measured by qRT-PCR. Data are shown as mean fold change±s.e.m. for *MEST* expression relative to control lines at cycle 0. A two-way ANOVA analysis was performed to show a significant difference in sample groups ($P<0.0001$) for gene expression between the groups of MSC lines followed by a Student's t-test ($^{*}P<0.05$). (D) EMSA with human recombinant SOX6 protein at increasing concentrations and a *MEST* promoter-based oligonucleotide encompassing site CpG B, either methylated or unmethylated and harboring a putative SOX6 binding site.

of this region in the SGA group of adipocyte cell lines was accompanied by increased expression of *MEST* (Fig. 4C), indicating a functional relationship between CpG methylation and gene expression levels in the two groups.

To examine the mechanistic basis for the above relationship, we conducted electrophoretic mobility shift assays (EMSAs) comparing methylated and non-methylated *MEST* probes covering the CpG B site next to a SOX6 binding motif. We found that CpG methylation at this site interferes with SOX6 binding (Fig. 4D), which might explain the lower expression of MEST in adipocytes from normal control MSCs and enhanced SOX6 binding in adipocytes from SGA neonates.

SOX6 inhibits WNT/β-catenin signaling in adipocytes

We observed that SOX6 promotes MEST expression and that SOX6 expression increases during adipocyte differentiation. We therefore investigated the possibility of SOX6 regulating the WNT signaling pathway, and showed that ectopic expression of SOX6 attenuates WNT3A-CM (conditioned medium)-mediated reporter activity (Fig. 5A). We demonstrated an interaction between β-catenin and SOX6 by co-immunoprecipitation (Fig. 5B,C). Furthermore, decreasing SOX6 expression in 3T3L1 cells during differentiation increased the levels of β-catenin protein (Fig. 5D). Similarly, treatment of cells with the specific proteasome inhibitor MG132 abolished the SOX6-mediated reduction in total cellular β-catenin levels and increased protein expression from its transcriptional target *Axin2* (Fig. 5E). These findings indicate that SOX6 depletion may alleviate suppression of the canonical β-catenin branch of the WNT signaling pathway by promoting proteasomal degradation of β-catenin.

SOX6 regulates lipid metabolism *in vivo*

In order to further establish the role of SOX6 in mediating adipogenesis *in vivo*, we investigated the effect of reducing SOX6 levels in C57BL/6 mice using locked nucleic acid antisense oligonucleotides (LNA ASOs). *Sox6*-specific ASO treatment was

Development (2016) 143, 950-961 doi:10.1242/dev.131573

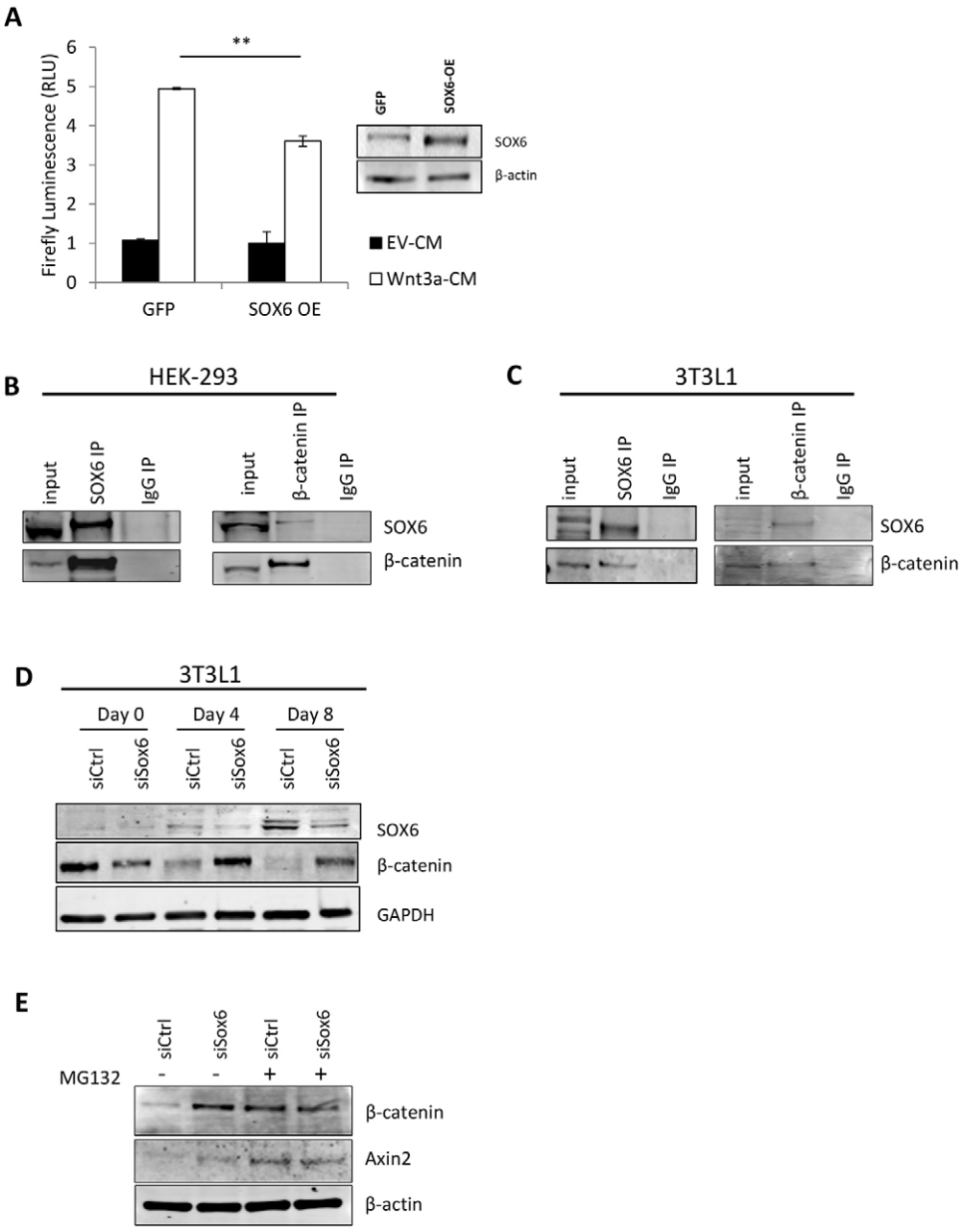

Fig. 5. Regulation of the WNT pathway by SOX6. (A) SOX6 inhibits TOP-FLASH activity induced by WNT3A-conditioned medium (WNT3A-CM). HEK293 cells co-transfected with a GFP or SOX6 expression plasmid (SOX6 OE) and TOP-FLASH reporter were incubated with the empty vector-conditioned medium (EV-CM) or WNT3A-CM for 16 h, followed by luciferase assays (left). Data are shown as mean luminescence (RLU)±s.e.m. compared with cells in EV-CM. $^{**}P<0.01$, two-way ANOVA. To the right is a western blot showing the expression of SOX6 protein after transfection. (B,C) Immunoprecipitations from HEK293 cells with ectopic SOX6 expression (B) or mouse 3T3L1 cells (C) with SOX6 antibody (left) or β-catenin antibody (right) show association of β-catenin with SOX6. Controls were samples immunoprecipitated with preimmune mouse or rabbit IgG (IgG). IP, immunoprecipitating antibody. (D) siRNA-mediated downregulation of SOX6 leads to an increase in β-catenin protein expression in 3T3L1 differentiated adipocytes. (E) The reduction of β-catenin protein by SOX6 in 3T3L1 adipocytes is based on proteasomal degradation. Alteration of β-catenin and AXIN2 protein levels by *Sox6* siRNA in the presence of 2 µM proteasome inhibitor MG132 versus its absence.

effective in decreasing *Sox6* mRNA expression in epididymal white adipose tissue (EWAT) and significantly decreased the expression of *Pparg*, *C/ebpa* and adiponectin (Fig. 6A). We also confirmed the *Sox6* knockdown in liver and EWAT (Fig. 6B, Fig. S5A,B). We then measured the lipid profiles and observed that *Sox6* ASO treatment reduced serum and liver triglyceride (Fig. 6C, D) as well as serum cholesterol levels (Fig. 6E). Serum levels of several adipokines, including leptin and adiponectin, correlate with adiposity and imbalances in their secretion may promote obesity-associated metabolic changes (Maury and Brichard, 2010). Serum leptin levels were significantly reduced in *Sox6* ASO-treated mice (Fig. 6F), consistent with the known positive correlation of leptin levels with fat mass (Considine et al., 1996). Serum levels of adiponectin, however, were not found to be significantly different in the *Sox6* ASO-treated mice compared with the controls (Fig. 6G), suggesting that adiponectin secretion in the blood serum does not contribute to the metabolic phenotype of SOX6-deficient mice.

To identify additional downstream target genes of SOX6 in the liver, we conducted a gene expression microarray study comparing livers from the control and *Sox6* ASO-treated mice for future validation of liver-specific functions of SOX6. From the microarray data set we selected the most significantly expressed genes and validated their expression levels by qRT-PCR. We confirmed upregulation of *Mknk2* and *Upp2* ($P\leq0.001$), as well as significant downregulation of *Pmvk*, *Fabp5*, *Immp2l*, *Nfat5*, *Dapk1*, *Ube2e1*, *Acss2*, *Acacb* and *Fasn* ($P\leq0.001$; Fig. S5C).

Loss of Sox6 decreases adipogenesis in zebrafish larvae

To address the potential conservation of Sox6 function in adipocyte differentiation across vertebrate species, we used zebrafish as an experimental model. The optical transparency of the zebrafish larva facilitates the visualization of adipocytes by Nile Red staining in whole-mount preparations (Flynn et al., 2009). Loss of Sox6 function in zebrafish has previously been shown to disrupt the differentiation of fast-twitch skeletal muscle fibers, but effects on

Development (2016) 143, 950-961 doi:10.1242/dev.131573

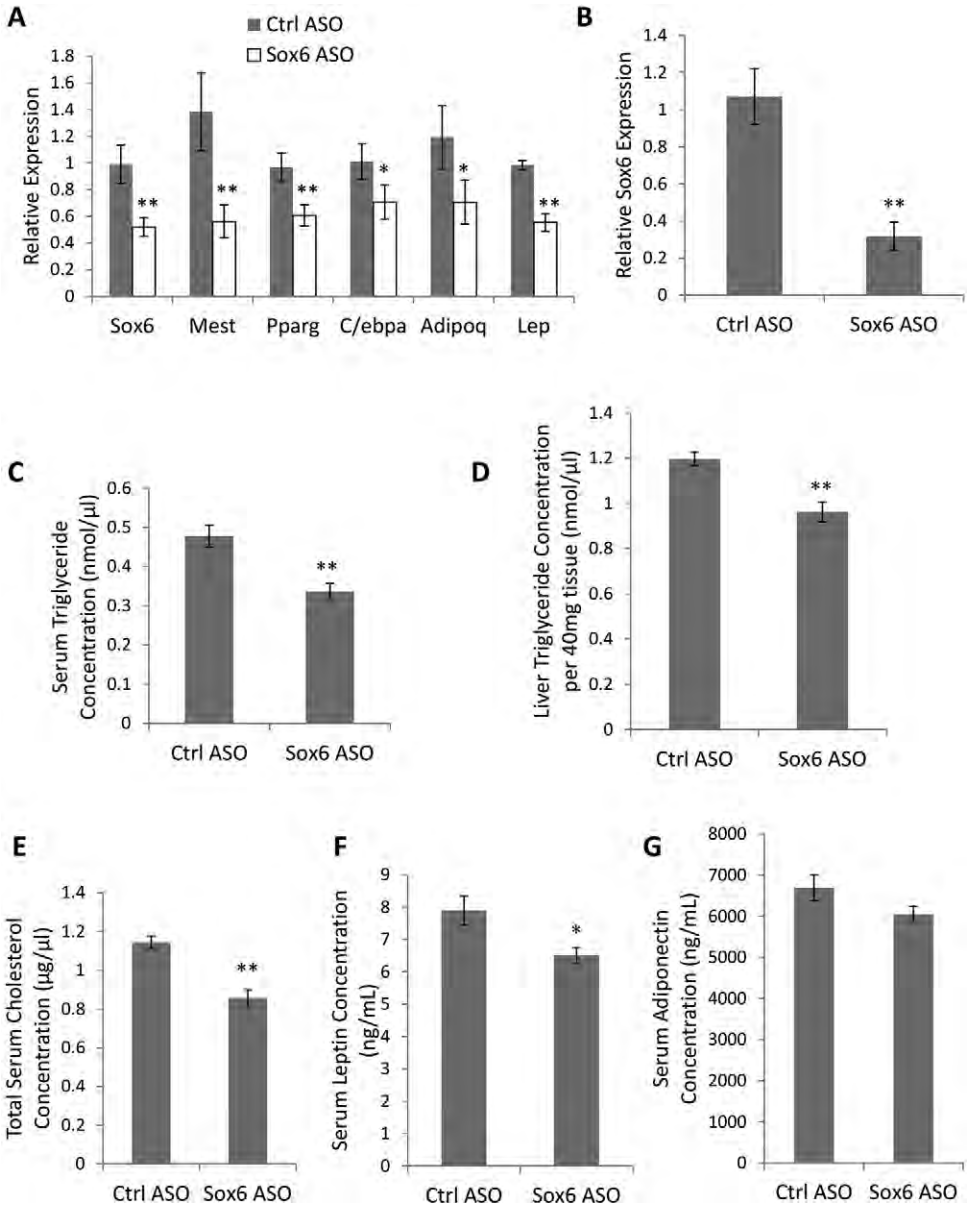

Fig. 6. Decreased lipid levels in mice following *Sox6* ASO treatment. (A) Mice (n=9 animals per group) on a chow diet were treated with control or *Sox6* ASO (50 mg/kg/week) by i.p. injection for a week. mRNA expression of *Sox6* and selected adipogenic genes in EWAT after ASO treatment. (B) mRNA expression of *Sox6* in the liver of ASO-treated mice. (C-E) Serum and liver triglyceride as well as serum cholesterol levels are reduced in mice treated with *Sox6* ASOs. (F,G) Serum levels of leptin and adiponectin levels in control and *Sox6* ASO-treated mice. Data are presented as mean±s.e.m. $^{**}P<0.01$, $^{*}P<0.05$, Student's t-test.

adipocytes have not been addressed (Jackson et al., 2015). For the current study, control and *sox6* homozygous null mutant larvae were stained with Oil Red O (Fig. 7A) or Nile Red (Fig. 7B) to reveal the localization of adipocyte neutral lipid droplets. Lipid droplets were reduced both in number and size in the *sox6* mutants (Fig. 7A,B). The number of neutral lipid droplets was decreased in *sox6* null mutants at all developmental stages (Fig. 7C).

DISCUSSION

The process of adipogenesis has been well studied and most master regulators have been identified. These include PPARγ and various members of the C/EBP family of transcription factors (Lefterova et al., 2014). We have described, for the first time, that the transcription factor SOX6 acts as an activator of adipogenesis upstream of PPARγ and MEST by direct binding to, and activation of, their promoters. SOX6 is a group D member of the SOX family of proteins, which includes SOX5 and SOX13 (Lefebvre et al., 2001), with essential roles in cell differentiation as demonstrated in studies with myocytes (Hagiwara et al., 2007), oligodendrocytes (Stolt et al., 2006), chondrocytes (Smits et al., 2001), neurons (Batista-Brito et al., 2009) and erythroblasts (Dumitriu et al., 2006). Although a possible role in regulating insulin secretion in pancreatic β-cells has been reported (Iguchi et al., 2005), our data suggest a direct metabolic function for SOX6 in regulating the triglyceride content in white adipose and liver tissues. This effect is evolutionarily conserved among vertebrates, as our data from *sox6*$^{-/-}$ zebrafish show.

The mechanism of action may differ in a tissue-specific manner, but in adipocytes, in addition to the direct regulation of PPARγ and C/EBP expression, we showed that SOX6 inhibits WNT signaling by binding to β-catenin, potentially leading to its degradation (Fig. 8). Our data from differentiated adipocytes reveal that this interaction involves proteasomal degradation of β-catenin with subsequent inhibition of β-catenin/T-cell factor (TCF) signaling. As the WNT pathway is known to inhibit adipogenesis (Ross et al., 2000; Kennell and MacDougald, 2005), SOX6 therefore counteracts this negative influence and promotes adipocyte differentiation. However, the interaction with β-catenin is not the only way in which SOX6 can act

Development (2016) 143, 950-961 doi:10.1242/dev.131573

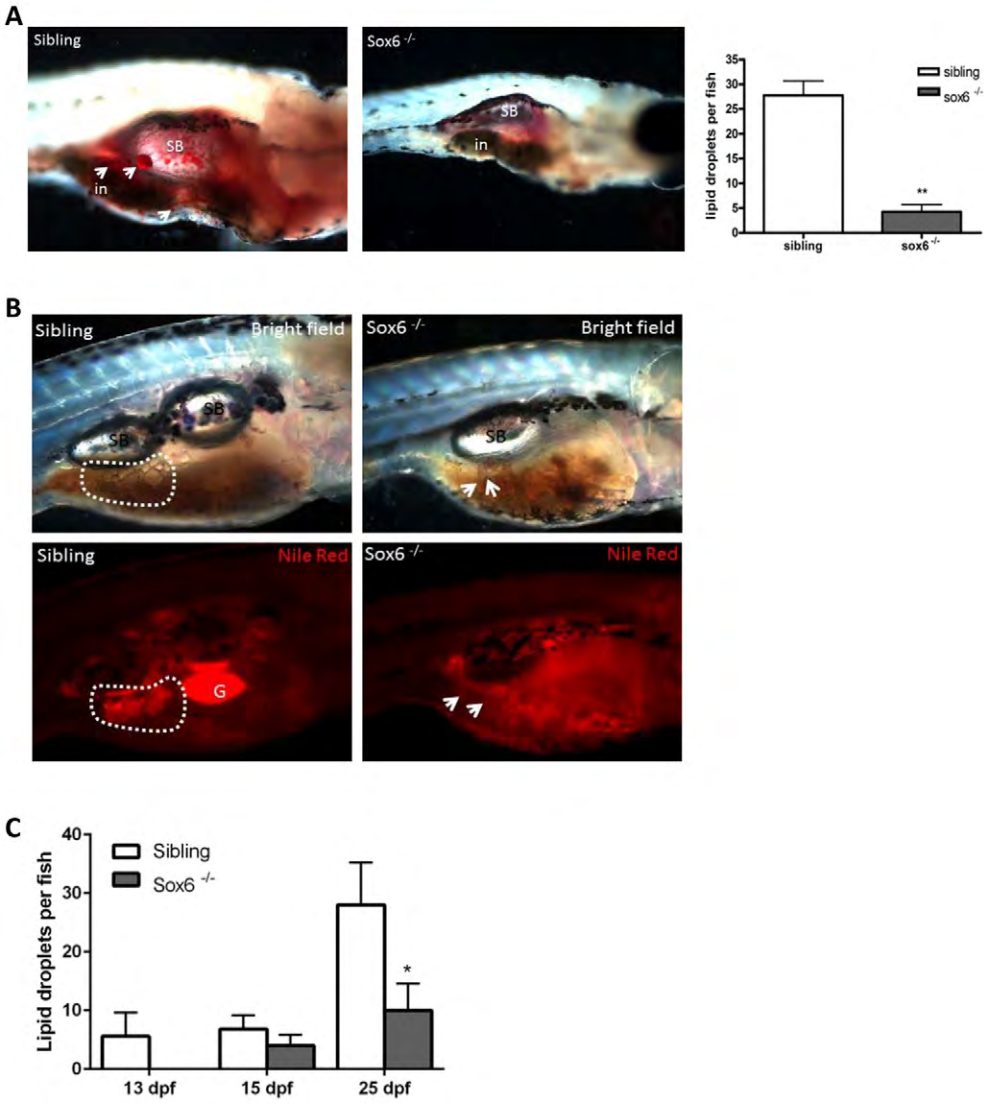

Fig. 7. *sox6* mutant zebrafish larvae exhibit decreased adipogenesis. (A) Oil Red O staining reveals localization of adipocyte neutral lipid droplets in larvae at 23 days post fertilization (dpf). The arrows indicate the localization of adipocytes. The number and the size of neutral lipid droplets are decreased in *sox6* mutants. Swim bladder (sb) and intestine (in) are indicated. Anterior is to the right and dorsal at the top in all images. Error bars represent s.d.; sibling $n=4$, mutant $n=4$; $^{**}P<0.01$, two-tailed unpaired Student's *t*-test. (B) Nile Red staining reveals that adipocyte lipid droplets are decreased in number and in size within the viscera of *sox6* mutant larvae at 25 dpf. Bright-field (upper panel) and corresponding fluorescence images (lower panel) are shown. Swim bladder (sb) and gall bladder (G) are indicated. The arrows indicate the localization of adipocytes (dotted line). (C) Live larvae at 13, 15 and 25 dpf were stained with Nile Red. The number of lipid droplets is decreased in *sox6* mutant larvae at all these developmental stages. Error bars represent s.d.; sibling $n=4$, mutant $n=4$; $^{*}P<0.05$, two-tailed unpaired Student's *t*-test.

upon WNT signaling. One of the key molecular associates of adipocyte size is the gene *MEST* and we identified a strong effect of SOX6 depletion on MEST expression levels, which can be explained by our data revealing direct binding of SOX6 to the *MEST* promoter. MEST has been reported to inhibit the WNT/β-catenin signaling pathway by sequestering β-catenin (Li et al., 2014) and through glycosylation of LRP6 (Jung et al., 2011). *MEST* (*PEG1*) is an imprinted gene that is expressed from the paternal allele (Kamei et al., 2007), and probable developmental functions of MEST could complement those of SOX6.

At present, we do not understand which factors promote SOX6 upregulation in SGA-derived adipocytes, apart from the strong association with hyperacetylated histones. But higher SOX6 expression levels in adipocytes from SGA individuals may synergize with *MEST* hypomethylation at CpGs found next to putative SOX6 binding sites. Decreased CpG methylation within the *MEST* promoter may facilitate SOX6 binding, thereby enhancing *MEST* expression, which in turn will stimulate lipogenesis and adipocyte growth. This model is supported by our EMSA data demonstrating impaired SOX6 binding to a *MEST* promoter template with adjacent CpG methylation. Our findings therefore extend published observations that obesity significantly associates with decreased methylation levels at the *MEST* gene (Soubry et al., 2015), that *MEST* hypomethylation is linked to metabolic programming in offspring with a background in gestational diabetes (El Hajj et al., 2013), and that there is an inverse relationship between *MEST* CpG methylation levels and body composition measures, such as waist circumference and body mass index (Carless et al., 2013).

We previously published observations of significant molecular changes in Wharton's jelly-derived MSCs from SGA infants prior to (Sukarieh et al., 2014) and post (Joseph et al., 2015) adipocyte differentiation. Given its evolutionary importance and demonstration in multiple species (Hanson and Gluckman, 2014), it seems probable that multiple molecular pathways operate to predispose individuals with a history of suboptimal early-life conditions to later increased metabolic disease risk. However, our study cannot conclusively prove a direct role for SOX6 in directing the fetal origins of human obesity but, in concert with other likely mechanisms, such as its direct effects on PPARγ expression and WNT signaling, SOX6 may be considered a key candidate in such processes.

The basic functions of SOX6 in adipogenesis are conserved between humans and other vertebrates, as shown by our cell line (mouse 3T3L1) and *in vivo* (mouse and zebrafish) data. Future research will address in more detail the mechanisms underlying the

Development (2016) 143, 950-961 doi:10.1242/dev.131573

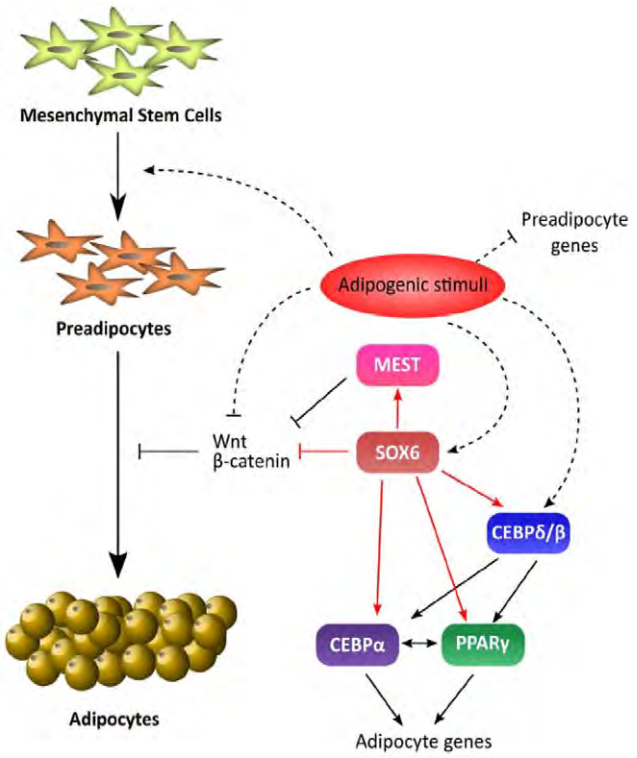

Fig. 8. Model of SOX6 regulation of adipogenesis. SOX6 activates adipogenesis by directly promoting the expression of C/EBP proteins and PPARγ. In addition, SOX6 binds to the *MEST* promoter to activate its expression, which in response inhibits WNT signaling. SOX6 also directly binds to β-catenin, leading to its degradation, which further blocks WNT signaling, promoting adipocyte differentiation.

dysregulation of SOX6 expression in the context of fetal growth restriction.

MATERIALS AND METHODS

Clinical populations and sample collection

Fresh UCs were obtained from children born at the National University Hospital (NUH), Singapore. Institutional Review Board (IRB) approval by the National University Health System (NUHS) was granted before cord collection. Prior written parental consent to participate in this study was obtained and ethical approval obtained by the Domain Specific Review Board (DSRB, # 2011/00355) of NUH.

Collection and establishment of human ASC lines

Prior written consent to participate in this study was obtained and ethical approval was granted by the Domain Specific Review Board (DSRB, #2013/00171) of NUH. Human subcutaneous white adipose tissue (WAT) was obtained from two morbidly obese patients who underwent either laparoscopic sleeve gastrectomy or Roux-en-Y gastric bypass (Table S1). The ASC lines APOD-01 and APOD-02 were established according to standard procedures. Briefly, less than 1 g WAT was digested with 1 mg/ml collagenase type IA (Sigma C9891-1G) in 20 mg/ml bovine serum albumin (BSA) for 90 min at 37°C with shaking (120 rpm). Cell pellets were collected by centrifugation at 800 ***g*** for 10 min, and then resuspended in 9 ml red blood cell (RBC) lysis buffer for 10 min. Cells were filtered through a 100 µm cell strainer and resuspended in growth medium comprising Dulbecco's modified Eagle's medium (DMEM)/F-12 GlutaMAX (Gibco) containing 20% fetal bovine serum (FBS) (Gibco 16000), 1% penicillin/streptomycin (Gibco 15140).

Assessment of fetal growth characteristics

Fetal growth characteristics were assessed by published methods (Sukarieh et al., 2014; Joseph et al., 2015). Briefly, the SGA condition was diagnosed by ultrasonography and determined as growth between the fifth and tenth percentile when compared with a control reference population. Standard scans were conducted by trained ultrasonographers, using ultrasound machines (Aloka SSD- 4000, GE Voluson E8).

Preparation and propagation of MSCs from human UC

The preparation and full characterization of the primary MSC isolates used in this study has been reported (Fong et al., 2010; Sukarieh et al., 2014; Joseph et al., 2015). A brief overview of the characteristics of all primary cell isolates used here is provided in Table S2. For all experiments described, the primary cell lines were passaged up to ten times.

Adipocyte differentiation

Wharton's jelly MSCs

The differentiation of MSCs is described by Joseph et al. (2015).

Human ASCs

Cells were plated in 3 cm or 6 cm dishes coated with 0.2% gelatin and grown in growth medium [DMEM/F-12 GlutaMAX, 20% FBS, antibiotic/antimycotic mixture (Gibco 15240-062)]. Two days after reaching confluence (day 0), the cells were stimulated to differentiate by culturing them in IBMX induction medium comprising DMEM/F-12 GlutaMAX, 10% FBS, supplemented with 0.5 mM isobutylmethylxanthine (IBMX, Sigma I-7018), 1 µM dexamethasone (Sigma D-4902), 200 µM indomethacine (Sigma I-8280) and 58 µg/ml insulin (bovine, Sigma I-5500), for 1 week with replacement by fresh medium every 2 days. After 1 week, the IBMX induction medium was replaced with insulin medium comprising DMEM/F-12 GlutaMAX, 10% FBS, supplemented with 0.01 mg/ml insulin. The insulin medium was changed every 2 days. The siRNA knockdown was performed before differentiation and every 4 days during differentiation.

Mouse 3T3L1 cells

Cells were obtained from ATCC and plated in 3 cm or 6 cm dishes coated with 0.2% gelatin and grown in growth medium (DMEM high glucose with 2 mM L-glutamine, 10% FBS, antibiotic/antimycotic mixture) and allowed to grow to confluence for 2-3 days. The cells were then treated with induction medium comprising DMEM high glucose with 2 mM L-glutamine, 10% FBS, supplemented with 0.5 mM IBMX, 1 µM dexamethasone, 0.01 mg/ml insulin (day 0) for 48 h. After 48 h, the induction medium was replaced with insulin medium comprising DMEM high glucose with 2 mM L-glutamine, 10% FBS, 0.01 mg/ml insulin. The insulin medium was changed every 2 days.

Oil Red O staining

Adipogenesis was quantified by Oil Red O staining following standard procedures. The adipogenic cultures in 3 cm dishes were washed with PBS and fixed with 10% formaldehyde for 30-60 min at room temperature. Oil Red O stock solution [0.3 g powder (Sigma O0625) in 100 ml isopropanol] was mixed 3:2 with deionized water and left at room temperature for 10 min before filtering. The Oil Red O solution was added to the dishes for 10 min at room temperature.

For whole-mount zebrafish staining, larvae were fixed with 4% paraformaldehyde (PFA), rinsed with PBT (PBS with 0.5% Tween 20), and stained with the filtered Oil Red O solution for 15 min at room temperature. Stained larvae were rinsed three times with PBT and twice with 60% isopropanol for 5 min each, then briefly rinsed with PBT and refixed with 4% PFA for 10 min. Finally, the larvae were mounted in 3% methylcellulose and imaged using an AxioCam HRc mounted on an Axio Imager M2 (Zeiss).

Nile Red staining

Nile Red (Wako 144-0811) was dissolved in acetone at 1.25 mg/ml and kept at −20°C in the dark. Live zebrafish were placed in egg water containing 0.5 µg/ml Nile Red for 30 min in the dark. Zebrafish were then anesthetized using tricaine (Sigma-Aldrich MS-222) and mounted in 3% methylcellulose for imaging as above.

Development (2016) 143, 950-961 doi:10.1242/dev.131573

ChIP-seq of histone H3K27 acetylation and methylation and bioinformatics analysis

All procedures for the ChIP-seq study, including all analytical steps, were as published (Joseph et al., 2015). The ChIP-seq data are available at the GEO repository (GSE64697).

ChIP

To preserve protein-DNA complexes, 1% formaldehyde was added to the cells for 10 min at room temperature. The cross-linking reactions were stopped by adding 125 mM glycine for 5 min and cells were incubated in SDS lysis buffer and sonicated (Diagenode Bioruptor) for 12 min. Chromatin fragments were precleared with protein A-Sepharose beads (Invitrogen 10-1142) and BSA at 4°C for 2 h prior to immunoprecipitation with 5 µg SOX6 antibody (Abcam ab30455) or 5 µg rabbit IgG control antibody (Santa Cruz sc-2027) overnight at 4°C. After washing and eluting the Sepharose beads with SDS elution buffer, the cross-links were reversed at 65°C overnight. The QIAquick PCR Purification Kit (Qiagen) was used for sample purification following the manufacturer's instructions.

Quantitative ChIP-PCR analysis

For the data shown in Fig. 3E, *MEST* and *PPARG* promoter-specific primers (Table S3) were used to analyze ChIP enrichment using the ABI 7900 system (PerkinElmer).

Co-immunoprecipitation assay

Cells were washed with ice-cold PBS and then lysed in 50 mM Tris (pH 8), 150 mM NaCl, 0.5% NP40, 0.5% deoxycholic acid, 0.005% SDS and protease inhibitors for 30 min on ice. Samples were centrifuged and the supernatants incubated with anti-SOX6 (Abcam ab125196; used at 2 µg/ml lysate), anti-β-catenin (BD Transduction Laboratories 610153; used at 2 µg/ml lysate), or rabbit IgG (Santa Cruz sc-2027; used at 2 µg/ml lysate) or mouse IgG (Santa Cruz sc-2025; used at 2 µg/ml lysate) control antibodies overnight at 4°C and with protein G-Sepharose beads (Invitrogen 10-1243) for 2 h. Beads were washed up to four times with 500 µl PBS, 0.1% Tween 20. SDS sample buffer was used to elute all bound proteins, which were then separated by SDS-PAGE followed by immunoblotting with the specific antibodies stated.

RNA extraction

Cells were spun down [1000 rpm (207 ***g***), 3 min] in 1.7 ml tubes and resuspended in 0.5 ml TRIzol reagent (Life Technologies 15596-026). Samples were snap-frozen on dry ice and stored at −80°C. RNA was isolated and purified using the RNeasy Mini Kit (Qiagen 74106) following the manufacturer's protocol.

Quantitative real-time PCR

For qRT-PCR, total RNA (1-2 µg) was reverse transcribed using the High Capacity cDNA Reverse Transcription Kit (Applied Biosystems). cDNA samples were subjected to real-time PCR analysis (in triplicate) with gene-specific primers (Table S3) using an ABI 7900 HT Sequence Detection System (Applied Biosystems). Target gene expression levels were normalized to endogenous control genes (*GAPDH* or *Ppia*) and presented relative to the controls.

Animal studies

Rodents

C57BL/6NTac mice were purchased from BRC, A*STAR. All experimental procedures were approved by the Institutional Animal Care and Use Committee (IACUC). All mice were monitored daily for signs of morbidity. Whole blood was collected by cardiac puncture. For tissue collection, the mice were sacrificed according to IACUC guidelines, and EWAT and liver were collected for analysis.

Zebrafish

A 14 h light/10 h dark cycle at 28°C in the AVA (Singapore) certificated IMCB Zebrafish Facility was employed for the maintenance of adult fish. The zebrafish strain used was Sox6i292 (Jackson et al., 2015).

ASO *in vivo* administration

Lyophilized LNA ASOs were produced according to Exiqon proprietary design software and dissolved in sterile water. The sequences (5′-3′) for the ASOs used are: negative control, AACACGTCTATACGC; *SOX6* sequence, TCTAGGTGGATTTTGC. ASOs were then diluted in saline to the desired concentration for dosing mice and sterilized through a 0.2 µm filter. Mice were anesthetized with Avertin before ASOs were delivered via intraperitoneal (i.p.) injection at 50 mg/kg per week. After 1 week, mice were sacrificed for blood and tissue collection.

Quantification of triglyceride content

Total soluble lipids from adipocytes differentiated from MSCs and 3T3L1 cells were extracted using the buffer provided with the commercial Adipogenesis Detection Kit (Abcam ab102513) and samples stored at −80°C until analysis. Triglycerides were quantified using the Triglyceride Quantification Kit (Abcam ab65336) as per the manufacturer's instructions.

Quantification of cholesterol

Whole blood was obtained from mice by cardiac puncture. Blood was stored in Sarstedt S-Monovette tubes containing serum gel. Serum was obtained by centrifuging the tubes at 10,000 ***g*** at room temperature for 10 min. Liver samples from mice were snap-frozen and kept at −80°C until analysis. Total cholesterol was measured using the Cholesterol/Cholesteryl Ester Quantification Kit (Abcam ab65359) using a colorimetric method as per the manufacturer's instructions.

Quantification of leptin and adiponectin

Serum levels of leptin and adiponectin were determined using ELISA, as per the manufacturer's instructions (R&D Systems, MOB00, MRP300).

Western blotting

Differentiated adipocytes were harvested in RIPA buffer (50 mM Tris-HCl pH 7.4, 150 mM NaCl, 2 mM EDTA, 1% NP-40, 0.1% SDS). Membranes were probed with primary antibodies specific to SOX6 (Abcam ab125196; 1:1000), MEST (Abcam ab151564; 1:1000), β-catenin (BD Transduction Labs 610153; 1:1000), AXIN2 (Abcam ab109307; 1:500), PPARγ (Santa Cruz sc7196; 1:1000), C/EBPα (Santa Cruz sc61; 1:1000), FABP4 (Abcam ab66682; 1:1000) and the endogenous control protein β-actin (Sigma A1978; 1:10,000). To inhibit proteasome-mediated protein degradation, 2 µM MG132 (Sigma C2211) was added to the cells. The LI-COR Odyssey 2.1 system was used for signal detection (secondary antibodies LI-COR 926-32211, 926-68020) and band analysis.

SOX6 siRNA knockdown studies

SOX6 was knocked down before differentiation and before each cycle of the adipocyte induction process in insulin medium using ON-TARGETplus Human SOX6 siRNA SMARTpool (Dharmacon L-015101-01-0050), ON-TARGETplus Mouse Sox6 siRNA SMARTpool (Dharmacon L0442910-01-0050) or ON-TARGETplus Non-targeting Pool siRNA (Dharmacon D-001810-10-50) at a final concentration of 100 nM. Transfections were conducted using Lipofectamine RNAiMAX (Invitrogen 13778150).

SOX6 overexpression study

For the overexpression of SOX6, mouse 3T3L1 cells were transfected using Lipofectamine LTX (Invitrogen) with 2.5 µg GFP-tagged plasmid containing the mouse *Sox6* gene (MG227129; Origene Technologies) in 6 cm dishes. This transient transfection was performed before differentiation and every 2 days during differentiation.

Luciferase reporter assay

For the WNT activity reporter assay, HEK293 cells were cultured in growth medium (DMEM high glucose with 2 mM L-glutamine, 10% FBS, antibiotic/antimycotic mixture). Cells seeded in 6-well plates were co-transfected with 1 µg SuperTOP-FLASH (Addgene plasmid #12456), 100 ng pTK-Renilla luciferase (Promega E2241) and 1.5 µg GFP-tagged plasmid containing the human *SOX6* gene (Origene Technologies RG211525). For the PPARγ reporter assay, 3T3L1 cells were co-

Development (2016) 143, 950-961 doi:10.1242/dev.131573

transfected with 1 µg PPRE-X3-TK-luc (Addgene plasmid #1015) and 100 ng pTK-Renilla luciferase. All assays were conducted following the Dual-Luciferase Assay protocols (Promega E1910). TOP-FLASH activity was normalized against Renilla luciferase readout. For the MEST reporter assay, 3T3L1 cells were co-transfected with 1 µg custom-made GLuc_ON *MEST* promoter reporter using pEZX-PG04 vector (GeneCopoeia MPRM26666-PG04). Assays were performed according to the Secrete-Pair Gaussia Luciferase Dual Assay Kit (GeneCopoeia SPDA-D010). Secreted alkaline phosphatase luciferase activity was used to normalize Gaussia luciferase (GLuc)-*MEST* promoter activity.

Pyrosequencing

Genomic DNA was prepared and converted with bisulfite using the EpiTect Bisulfite Kit (Qiagen) according to the manufacturer's recommendations. Pyrosequencing was performed using a PyroMark Q24 machine (Qiagen) in 10-15 µl PCR product in a standard reaction volume. PCR and sequencing primers are provided in Table S3.

EMSA

EMSA was performed using the Odyssey Infrared EMSA Kit (LI-COR 829-07910). Varying concentrations of human recombinant SOX6 protein (Origene TP312046) were incubated for 20 min at room temperature with a synthetic *SOX6* oligonucleotide 5′ end-labeled with IRDye 700 (Integrated DNA Technologies) with or without 5-methyl-dC modification at the CpG motif (double stranded, 5′-TTATTCTCTTTATCCAATGCCGGAGGCTAT-3′) and a binding mix following the manufacturer's protocol. Separation of reaction products was performed on a 6% non-denaturing polyacrylamide gel in 0.5× cold TBE buffer (pH 8).

Gene expression microarray

Differential gene expression levels in liver tissue comparing *SOX6* and control ASOs were determined by employing HumanHT-12 v4 Expression BeadChip technology (Illumina BD-103-0204). The Illumina iScan system was used for scanning the arrays followed by data extraction using Illumina Genome Bead Studio Software. After background subtraction, *P*-values <0.05 and NBEADS >3 using the R program were determined. The data were further analyzed with Arraystudio (Omicsoft). Probes that passed signal detected $P<0.05$ in all the samples were retained. Log_2 transformation (intensity values <1 censored to 0) was performed followed by quantile normalization. One-way ANOVA (~*t*-test) was performed to determine differential gene expression. Gene expression microarray data are available at GEO under accession number GSE70300.

Statistics

Data are generally presented as mean±s.e.m. Comparisons between groups and time courses [e.g. the adipogenesis differentiation assays involving different stages (cycles)] were analyzed by repeated measures analysis of variance (ANOVA). All normal comparisons between groups were assessed using Student's *t*-test, with $P<0.05$ considered significant.

Acknowledgements

We are grateful for the expert technical assistance of Jun Hao Tan, Maggie Lim, Ge Xiaojia and Sathiakumar Durgalakshmi.

Competing interests

The authors declare no competing or financial interests.

Author contributions

S.C.L.: performed the experiments, conception and design, data collection and analysis and interpretation; J.P., P.G.T., J.Y., R.J., C.M., S.P.: performed the experiments, data collection and analysis; S.D.: data analysis; A.S., K.L.N., P.W.I., M.K.S.L., Y.S.L., Y.S.C., P.D.G.: clinical and biological specimen collection, manuscript editing; W.S.: conception and design, data analysis, manuscript writing.

Funding

This research is supported by the Singapore National Research Foundation under its Translational and Clinical Research (TCR) Flagship Programme and administered by the Singapore Ministry of Health's National Medical Research Council (NMRC), Singapore [NMRC/TCR/004-NUS/2008, NMRC/TCR/012-NUHS/2014]. Singapore Institute for Clinical Sciences investigators are supported through Agency for Science Technology and Research (A*STAR) funding.

Supplementary information

Supplementary information available online at
http://dev.biologists.org/lookup/suppl/doi:10.1242/dev.131573/-/DC1

References

Batista-Brito, R., Rossignol, E., Hjerling-Leffler, J., Denaxa, M., Wegner, M., Lefebvre, V., Pachnis, V. and Fishell, G. (2009). The cell-intrinsic requirement of Sox6 for cortical interneuron development. *Neuron* **63**, 466-481.

Bhurosy, T. and Jeewon, R. (2014). Overweight and obesity epidemic in developing countries: a problem with diet, physical activity, or socioeconomic status? *Sci. World J.* **2014**, 964236.

Carless, M. A., Kulkarni, H., Kos, M. Z., Charlesworth, J., Peralta, J. M., Göring, H. H. H., Curran, J. E., Almasy, L., Dyer, T. D., Comuzzie, A. G. et al. (2013). Genetic effects on DNA methylation and its potential relevance for obesity in Mexican Americans. *PLoS ONE* **8**, e73950.

Cho, H.-M., Lee, H.-A., Kim, H. Y., Lee, D.-Y. and Kim, I. K. (2013). Recruitment of specificity protein 1 by CpG hypomethylation upregulates Na^+;K^+-2Cl^- cotransporter 1 in hypertensive rats. *J. Hypertens.* **31**, 1406-1413.

Considine, R. V., Sinha, M. K., Heiman, M. L., Kriauciunas, A., Stephens, T. W., Nyce, M. R., Ohannesian, J. P., Marco, C. C., McKee, L. J., Bauer, T. L. et al. (1996). Serum immunoreactive-leptin concentrations in normal-weight and obese humans. *N. Engl. J. Med.* **334**, 292-295.

de Rooij, S. R., Painter, R. C., Holleman, F., Bossuyt, P. M. and Roseboom, T. J. (2007). The metabolic syndrome in adults prenatally exposed to the Dutch famine. *Am. J. Clin. Nutr.* **86**, 1219-1224.

Desai, M., Gayle, D., Babu, J. and Ross, M. G. (2005). Programmed obesity in intrauterine growth-restricted newborns: modulation by newborn nutrition. *Am. J. Physiol. Regul. Integr. Comp. Physiol.* **288**, R91-R96.

Dumitriu, B., Patrick, M. R., Petschek, J. P., Cherukuri, S., Klingmuller, U., Fox, P. L. and Lefebvre, V. (2006). Sox6 cell-autonomously stimulates erythroid cell survival, proliferation, and terminal maturation and is thereby an important enhancer of definitive erythropoiesis during mouse development. *Blood* **108**, 1198-1207.

El Hajj, N., Pliushch, G., Schneider, E., Dittrich, M., Müller, T., Korenkov, M., Aretz, M., Zechner, U., Lehnen, H. and Haaf, T. (2013). Metabolic programming of MEST DNA methylation by intrauterine exposure to gestational diabetes mellitus. *Diabetes* **62**, 1320-1328.

Flynn, E. J., III, Trent, C. M. and Rawls, J. F. (2009). Ontogeny and nutritional control of adipogenesis in zebrafish (Danio rerio). *J. Lipid Res.* **50**, 1641-1652.

Fong, C.-Y., Subramanian, A., Biswas, A., Gauthaman, K., Srikanth, P., Hande, M. P. and Bongso, A. (2010). Derivation efficiency, cell proliferation, freeze-thaw survival, stem-cell properties and differentiation of human Wharton's jelly stem cells. *Reprod. Biomed.* **21**, 391-401.

Godfrey, K. M. and Barker, D. J. P. (2001). Fetal programming and adult health. *Public Health Nutr.* **4**, 611-624.

Godfrey, K. M., Sheppard, A., Gluckman, P. D., Lillycrop, K. A., Burdge, G. C., McLean, C., Rodford, J., Slater-Jefferies, J. L., Garratt, E., Crozier, S. R. et al. (2011). Epigenetic gene promoter methylation at birth is associated with child's later adiposity. *Diabetes* **60**, 1528-1534.

Hagiwara, N., Yeh, M. and Liu, A. (2007). Sox6 is required for normal fiber type differentiation of fetal skeletal muscle in mice. *Dev. Dyn.* **236**, 2062-2076.

Hanson, M. A. and Gluckman, P. D. (2014). Early developmental conditioning of later health and disease: physiology or pathophysiology? *Physiol. Rev.* **94**, 1027-1076.

Iguchi, H., Ikeda, Y., Okamura, M., Tanaka, T., Urashima, Y., Ohguchi, H., Takayasu, S., Kojima, N., Iwasaki, S., Ohashi, R. et al. (2005). SOX6 attenuates glucose-stimulated insulin secretion by repressing PDX1 transcriptional activity and is down-regulated in hyperinsulinemic obese mice. *J. Biol. Chem.* **280**, 37669-37680.

Jackson, H. E., Ono, Y., Wang, X., Elworthy, S., Cunliffe, V. T. and Ingham, P. W. (2015). The role of Sox6 in zebrafish muscle fiber type specification. *Skelet. Muscle* **5**, 2.

Joseph, R., Poschmann, J., Sukarieh, R., Too, P. G., Julien, S. G., Xu, F., Teh, A. L., Holbrook, J. D., Ng, K. L., Chong, Y. S. et al. (2015). ACSL1 is associated with fetal programming of insulin sensitivity and cellular lipid content. *Mol. Endocrinol.* **29**, 909-920.

Jung, H., Lee, S. K. and Jho, E.-H. (2011). Mest/Peg1 inhibits WNT signalling through regulation of LRP6 glycosylation. *Biochem. J.* **436**, 263-269.

Kamei, Y., Suganami, T., Kohda, T., Ishino, F., Yasuda, K., Miura, S., Ezaki, O. and Ogawa, Y. (2007). Peg1/Mest in obese adipose tissue is expressed from the paternal allele in an isoform-specific manner. *FEBS Lett.* **581**, 91-96.

Kennell, J. A. and MacDougald, O. A. (2005). WNT signaling inhibits adipogenesis through beta-catenin-dependent and -independent mechanisms. *J. Biol. Chem.* **280**, 24004-24010.

Development (2016) 143, 950-961 doi:10.1242/dev.131573

Kensara, O. A., Wooton, S. A., Phillips, D. I. W., Patel, M., Hoffman, D. J., Jackson, A. A., Elia, M. and Hertfordshire Study Group. (2006). Substrate-energy metabolism and metabolic risk factors for cardiovascular disease in relation to fetal growth and adult body composition. *Am. J. Physiol. Endocrinol. Metab.* **291**, E365-E371.

Khandelwal, P., Jain, V., Gupta, A. K., Kalaivani, M. and Paul, V. K. (2014). Association of early postnatal growth trajectory with body composition in term low birth weight infants. *J. Dev. Orig. Health Dis.* **5**, 189-196.

Lackland, D. T., Bendall, H. E., Osmond, C., Egan, B. M. and Barker, D. J. P. (2000). Low birth weights contribute to the high rates of early-onset chronic renal failure in the southeastern United States. *Arch. Intern. Med.* **160**, 1472-1476.

Lefebvre, V., Behringer, R. R. and de Crombrugghe, B. (2001). L-Sox5, Sox6 and Sox9 control essential steps of the chondrocyte differentiation pathway. *Osteoarthritis Cartilage* **9**, S69-S75.

Lefterova, M. I., Haakonsson, A. K., Lazar, M. A. and Mandrup, S. (2014). PPARγ and the global map of adipogenesis and beyond. *Trends Endocrinol. Metab.* **25**, 293-302.

Li, W., Zhu, C., Li, Y., Wu, Q. and Gao, R. (2014). Mest attenuates CCl4-induced liver fibrosis in rats by inhibiting the WNT/β-catenin signaling pathway. *Gut Liver* **8**, 282-291.

Maury, E. and Brichard, S. M. (2010). Adipokine dysregulation, adipose tissue inflammation and metabolic syndrome. *Mol. Cell. Endocrinol.* **314**, 1-16.

Ng, M., Fleming, T., Robinson, M., Thomson, B., Graetz, N., Margono, C., Mullany, E. C., Biryukov, S., Abbafati, C., Abera, S. F. et al. (2014). Global, regional, and national prevalence of overweight and obesity in children and adults during 1980–2013: a systematic analysis for the Global Burden of Disease Study 2013. *Lancet* **384**, 766-781.

Rosen, E. D., Hsu, C.-H., Wang, X., Sakai, S., Freeman, M. W., Gonzalez, F. J. and Spiegelman, B. M. (2002). C/EBPalpha induces adipogenesis through PPARgamma: a unified pathway. *Genes Dev.* **16**, 22-26.

Ross, S. E., Hemati, N., Longo, K. A., Bennett, C. N., Lucas, P. C., Erickson, R. L. and MacDougald, O. A. (2000). Inhibition of adipogenesis by WNT signaling. *Science* **289**, 950-953.

Smits, P., Li, P., Mandel, J., Zhang, Z., Deng, J. M., Behringer, R. R., de Crombrugghe, B. and Lefebvre, V. (2001). The transcription factors L-Sox5 and Sox6 are essential for cartilage formation. *Dev. Cell* **1**, 277-290.

Soubry, A., Murphy, S. K., Wang, F., Huang, Z., Vidal, A. C., Fuemmeler, B. F., Kurtzberg, J., Murtha, A., Jirtle, R. L., Schildkraut, J. M. et al. (2015). Newborns of obese parents have altered DNA methylation patterns at imprinted genes. *Int. J. Obes.* **39**, 650-657.

Stolt, C. C., Schlierf, A., Lommes, P., Hillgärtner, S., Werner, T., Kosian, T., Sock, E., Kessaris, N., Richardson, W. D., Lefebvre, V. et al. (2006). SoxD proteins influence multiple stages of oligodendrocyte development and modulate SoxE protein function. *Dev. Cell* **11**, 697-709.

Sukarieh, R., Joseph, R., Leow, S. C., Li, Y., Löffler, M., Aris, I. M., Tan, J. H., Teh, A. L., Chen, L., Holbrook, J. D. et al. (2014). Molecular pathways reflecting poor intrauterine growth are found in Wharton's jelly-derived mesenchymal stem cells. *Hum. Reprod.* **29**, 2287-2301.

Takahashi, M., Kamei, Y. and Ezaki, O. (2005). Mest/Peg1 imprinted gene enlarges adipocytes and is a marker of adipocyte size. *Am. J. Physiol. Endocrinol. Metab.* **288**, E117-E124.

Tian, J.-Y., Cheng, Q., Song, X.-M., Li, G., Jiang, G.-X., Gu, Y.-Y. and Luo, M. (2006). Birth weight and risk of type 2 diabetes, abdominal obesity and hypertension among Chinese adults. *Eur. J. Endocrinol.* **155**, 601-607.

van Dijk, S. J., Molloy, P. L., Varinli, H., Morrison, J. L., Muhlhausler, B. S. and Members of EpiSCOPE. (2015). Epigenetics and human obesity. *Int. J. Obes.* **39**, 85-97.

Varvarigou, A. A. (2010). Intrauterine growth restriction as a potential risk factor for disease onset in adulthood. *J. Pediatr. Endocrinol. Metab.* **23**, 215-224.

Vidal, A. C. Benjamin Neelon, S. E., Liu, Y., Tuli, A. M., Fuemmeler, B. F., Hoyo, C., Murtha, A. P., Huang, Z., Schildkraut, J., Overcash, F. et al. (2014). Maternal stress, preterm birth, and DNA methylation at imprint regulatory sequences in humans. *Genet. Epigenet.* **6**, 37-44.

Voigt, A., Ribot, J., Sabater, A. G., Palou, A., Bonet, M. L. and Klaus, S. (2015). Identification of Mest/Peg1 gene expression as a predictive biomarker of adipose tissue expansion sensitive to dietary anti-obesity interventions. *Genes Nutr.* **10**, 27.